Preprints of the 19th World Congress
The International Federation of Automatic Control
Cape Town, South Africa. August 24-29, 2014

A Curvilinear Abscissa Approach for the Lap Time Optimization of Racing Vehicles

R. Lot * **F. Biral** **

* *Department of Industrial Engineering, University of Padova, Italy (e-mail: roberto.lot@unipd.it).*
** *Department of Industrial Engineering, University of Trento, Italy (e-mail: francesco.biral@unitn.it)*

Abstract: The optimal control and lap time optimization of vehicles such as racing cars and motorcycle is a challenging problem, in particular the approach adopted in the problem formulation has a great impact on the actual possibility of solving such problem by using numerical techniques. This paper illustrates a methodology which combines some modelling technique which have been found to be numerically efficient. The methodology is based on the 3D curvilinear coordinates technique for the road modelling, the moving frame approach for the derivation of the vehicle equations of motion, the replacement of the time with the position along the track as new independent variable and the formulation and the solution of the minimum lap time problem by means of the indirect approach. The case study of a GT car is presented and simulation examples are given and discussed.

Keywords: Road modelling, racing vehicle, lap time optimization, curvilinear coordinates, optimal control

1. INTRODUCTION

The solution of minimum lap time problem is an important step of analysis in the racing industry. The problem is quite challenging due to the vehicle model complexity and the need to enforce path inequality constraints which yield a highly non linear system. In particular the path constraints that force the vehicle to run within the road boundaries have a great impact on the minimum lap time problem formulation complexity and consequently on the convergence rate. This is even more important when the elevation and road banking cannot be neglected. The present paper introduces a effective formulation in curvilinear coordinates for 3D roads which involves both road and vehicle modelling and allows fast and robust solution of optimal control problems like minimum lap time. Many different road modelling approaches have been proposed according to the type of simulation required. For off-road vehicle dynamic analysis a 3D mesh is commonly used to accurately model the terrain unevenness in a finite element method fashion. However, the calculation of the tyre contact point is time consuming Blundell and Harty (2004) despite the algorithms efficiency. In the past decade, it became more popular to define the road geometrical characteristics (i.e. curvature, elevation bank angle, friction coefficient) in tabular form by specifying the road centerline interpolated with piecewise functions between different data points Blundell and Harty (2004). This method is used by most software packages that are specific to vehicle analysis with slight differences. Nevertheless the curvilinear approach is only used to ease the road geometry description but it does not affect the equations describing the position and attitude of the vehicle with respect to the road which are still expressed in cartesian coordinates. This is the approach also used in many optimal control formulations for minimum lap time problem as described in Kirches et al. (2010), Braghin et al. (2008), Gerdts (2003) and Kelly and Sharp (2010). The cartesian coordinates approach involves quite complex equations to compute if a point is within the road boundaries. On the other hand in Cossalter et al. (1999) , Bertolazzi et al. (2005) for motorcycle dynamics and in Bertolazzi et al. (2007) , Kehrle et al. (2011) for four wheel vehicles it was proposed a model transformation from time-dependent to a 2D spatial/space road independent dynamics.
In this work the optimal control formulation is extended to a fully 3D road model which describes the vehicle dynamics with a moving frame (known also as Darboux frame Cui and Dai (2010)) with respect to a reference line located on a spatial surface. The vehicle equations of motions, described with respect to this frame, are symbolically derived and therefore linearization of small variables are possible when convenient. The overall system of equations is relatively simple and the vehicle position and orientation are fully described in term of road coordinates. The main advantage of the proposed formulation it is the natural implementation of road related path constraints which are also locally convex.

2. ROAD MODELLING

Real roads are similar to strips: they are long and narrow. Moreover, their extension in the ground horizontal plane is much greater than their vertical variations. According to these considerations, Fig. 1 illustrates a string-shaped road, which is defined by specifying the middle line $\mathcal{C}$, the direction of the lateral extension $\overrightarrow{\mathbf{n}}$ and the associated width w. The middle line $\mathcal{C}$ is defined by its cartesian coordinates w.r.t the inertial reference frame T_0 as a function of the parameter s:

$$\mathbf{C} = \{x(s), y(s), z(s)\}^T \tag{1}$$

Assuming that coordinate functions are normalized as follows:

$$x'(s)^2 + y'(s)^2 + z'(s)^2 = 1 \tag{2}$$

where the apex $'$ indicates the derivation with respect to s, the parameter s now assumes the meaning of *curvilinear abscissa* and corresponds to the length of the curve. The *banking* angle, i.e the angle between $\vec{\mathbf{n}}$ and the horizontal plane passing through $\mathbf{C}$, complete the road definition.
Let us now define a cartesian triad T_c with origin $\mathbf{C}$, axis x_c aligned with the unit vector $\vec{\mathbf{s}}$ tangent to $\mathcal{C}$ and axis y_c aligned with $\vec{\mathbf{n}}$. The orientation of T_c may be conveniently described by using a 3×3 rotation matrix Meirovitch (2010) defined by a sequence of rotations as follows:

$$\mathbf{R}_c = \mathbf{R}_z(\theta)\,\mathbf{R}_y(\sigma)\,\mathbf{R}_x(\beta) \tag{3}$$

where $\mathbf{R}_a$ is the rotation operator with respect to a cartesian axis $a \in \{x, y, z\}$. Angles θ, σ and β represent the road *heading* (i.e. the direction of travelling), *slope* (i.e. travelling up hill or down hill) and *banking* (i.e. the road leaning) respectively. For actual roads it is reasonable to assume that the banking and slope angles σ, β are infinitesimal [1] , consequently the rotation matrix $\mathbf{R}_c$ becomes:

$$\mathbf{R}_c = \begin{bmatrix} \cos(\theta) & -\sin(\theta) & \cos(\theta)\sigma + \sin(\theta)\beta \\ \sin(\theta) & \cos(\theta) & \sin(\theta)\sigma - \cos(\theta)\beta \\ -\sigma & \beta & 1 \end{bmatrix} \tag{4}$$

The columns of the rotation matrix correspond to the unit vectors along the cartesian axis Meirovitch (2010), in particular the first column corresponds to the unit vector $\vec{\mathbf{s}}$. But $\vec{\mathbf{s}}$ also corresponds to the gradient of $\mathcal{C}$, therefore:

$$x' = \cos(\theta) \tag{5a}$$
$$y' = \sin(\theta) \tag{5b}$$
$$z' = -\sigma \tag{5c}$$

The above differential equations are used to define the curve $\mathcal{C}$ not more by the triple of functions $x(s)$, $y(s)$, $z(s)$ constrained to equation (2), but with the couple of arbitrary functions $\theta(s), \sigma(s)$ and initial conditions $x(0)$, $y(0)$, $z(0)$. The banking angle $\beta(s)$ and strip width $w(s, n)$ complete the road description (the reader may note that the strip width can vary with s but also between left and right side). The road description is further improved by considering the skew symmetric tensor [2] Meirovitch (2010) $\mathbf{W}_c$ which describes the variation of the orientation of T_c as follows:

$$\mathbf{W}_c = \mathbf{R}_c'\,\mathbf{R}_c^T = \begin{bmatrix} 0 & -\kappa & \upsilon \\ \kappa & 0 & -\tau \\ -\upsilon & \tau & 0 \end{bmatrix} \tag{6}$$

where κ and υ correspond to the curvature of $\mathcal{C}$ in the *transversal* plane $x_c y_c$ and *sagittal* plane $x_c z_c$ respectively, while τ represent the *torsion* of the string. By substituting expression (4) into equation (6) and by rearranging terms, one obtains the above differential equations:

$$\theta' = \kappa \tag{7a}$$
$$\sigma' = \upsilon - \beta\kappa \tag{7b}$$
$$\beta' = \kappa\sigma + \tau \tag{7c}$$

which are used to replace angles functions by curvature functions in the definition of the road. In conclusion, the strip may be fully described by means of curvatures triple $\kappa(s), \upsilon(s), \sigma(s)$, initial coordinate $x(0), y(0), z(0)$, initial orientation $\theta(0), \sigma(0), \beta(0)$ and width $w(s)$.

[1] This assumption may be removed if necessary with an additional complexity of the obtained equations

[2] In the time domain this relation gives the well known velocity matrix $\mathbf{W} = \dot{\mathbf{R}}\,\mathbf{R}^T$

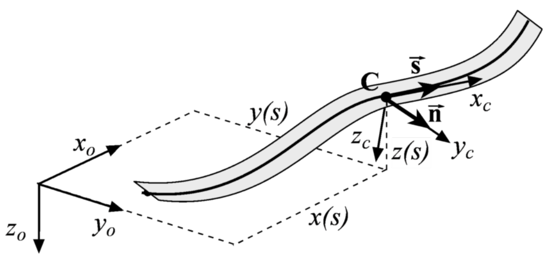

Fig. 1. Coordinates system of the strip-road model

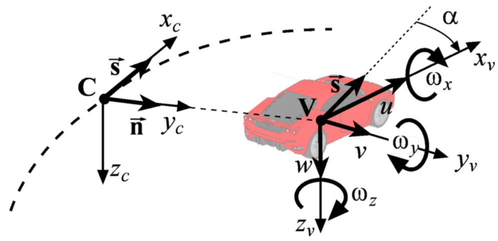

Fig. 2. Moving frame

3. VEHICLE MODELLING

To derive the equations of motion it is convenient to define a moving reference frame $\mathbf{T}_V$ as follows: the origin $\mathbf{V}$ is located at road level just below the vehicle center of mass, the axis z_v is orthogonal to the road surface, while the axis x_v is the intersection between the sagittal plane of the vehicle and the plane tangent to road surface, Fig. 2. The position of the point $\mathbf{V}$ on the road surface is defined by means of the curvilinear abscissa s (i.e. the position along the road) and lateral coordinate n, finally the relative yaw angle α defines the orientation of the x_v axis and complete the definition of the reference frame $\mathbf{T}_v$. According to this definition, the components of the velocity of point $\mathbf{V}$ expressed w.r.t. the reference frame $\mathbf{T}_V$ are:

$$u = [1 - n\kappa(s)]\dot{s}\cos\alpha + \dot{n}\sin\alpha \tag{8a}$$
$$v = -[1 - n\kappa(s)]\dot{s}\sin\alpha + \dot{n}\cos\alpha \tag{8b}$$
$$w = n\tau(s)\dot{s} \tag{8c}$$

Moreover, the components of the angular velocity of $\mathbf{T}_V$ w.r.t. itself axes are:

$$\omega_x = [\tau(s)\cos\alpha + \upsilon(s)\sin\alpha]\dot{s} \tag{9a}$$
$$\omega_y = [-\tau(s)\sin\alpha + \upsilon(s)\cos\alpha]\dot{s} \tag{9b}$$
$$\omega_z = \kappa(s)\dot{s} + \dot{\alpha} \tag{9c}$$

Since the road torsion $\tau(s)$ and sagittal curvature $\upsilon(s)$ have been assumed to be infinitesimal, according to equation (9a) and (9b) angular speeds ω_x, ω_y will be assumed infinitesimal too.
We extended the equations of motion of the well known 2D single track model Abe (2009) (Fig. 3) taking into account the front/rear load transfer and the road geometry

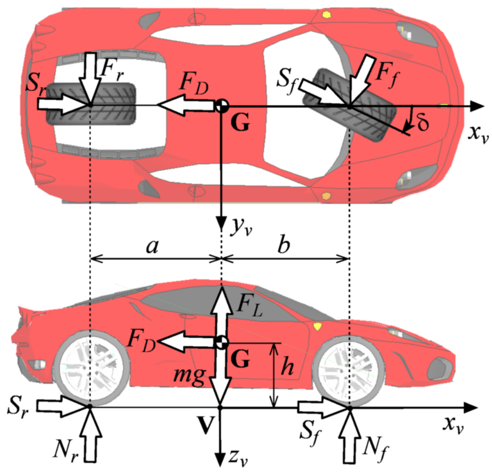

Fig. 3. Single track model with load transfer

above defined. Assuming that the road is locally flat and the steering angle δ is small, the translation Newton's equations w.r.t the moving frame $\mathbf{T}_V$ are:

$$M(\dot{u}+\omega_y w-\omega_z v)+Mg[\sigma(s)\cos\alpha-\beta(s)\sin\alpha] \\ +Mh(-\omega_x\omega_z-\dot{\omega}_y)=S_r+S_f-F_f\delta-F_D(u) \quad (10a)$$

$$M(\dot{v}-\omega_x w+\omega_z u)-Mg[\beta(s)\cos\alpha+\sigma(s)\sin\alpha] \\ +Mh(\dot{\omega}_x-\omega_y\omega_z)=F_r+F_f-S_f\delta \quad (10b)$$

$$M(\dot{w}-\omega_y u+\omega_x v)=Mg-F_L(u)-N_r-N_f \quad (10c)$$

where M is the vehicle mass, N, S, F are respectively the vertical, longitudinal and lateral force of tires, where the suffixes r, f indicate respectively the rear and front axles, F_D and F_L are respectively the aerodynamic drag and lift forces, which depend on the speed u according to the well know relations:

$$F_D=\frac{1}{2}\rho AC_D u^2, \qquad F_L=\frac{1}{2}\rho AC_L u^2 \quad (11a)$$

where ρ is the air density, A is the drag area, while C_D and C_L are respectively the drag and lift coefficients. It may be observed that gravity force terms in equations (10) depend on the road banking and slope, moreover banking and slope variations generate the acceleration terms which depend on ω_x, ω_y.
The following pitch and yaw equations complete the model:

$$I_{yy}\dot{\omega}_y+(I_{xx}-I_{zz})\omega_x\omega_z-I_{xz}\omega_z^2= \\ =aN_f-bN_r+h(S_r+S_f-F_f\delta) \quad (12a)$$

$$I_{zz}\dot{\omega}_z=-bF_r+a(F_f-S_f\delta) \quad (12b)$$

where I_{ij} are the element of the vehicle inertia tensor ($I_{xy}=I_{yz}=0$ for symmetry, while second order terms $\omega_y\omega_x$ are neglected).

According to Hans B. (2005) each tire lateral force F has been assumed to be proportional to the sideslip angle λ and tire load N as follows:

$$F_r=K_r\lambda_r N_r=K_r\frac{v-b\omega_z}{u}N_r \quad (13a)$$

$$F_f=K_f\lambda_r N_f=K_f\left[\delta\left(1+\frac{a^2\omega_z^2}{u^2}\right)-\frac{v+a\omega_z}{u}\right]N_f \quad (13b)$$

where K_r and K_f are respectively the rear and front sideslip cornering stiffness. It is worth pointing out that tire saturation will be included in the model afterwards as a constraint of the minimum lap time problem. Longitudinal forces are assumed to be control variables: the overall longitudinal force S is completely applied on the the rear axle in traction condition ($S>0$), while it is split between the front and rear axles in braking conditions ($S<0$) as follows:

$$S_f=\min(\varrho S,0)\ , \quad S_r=S-S_f \quad (14)$$

where ϱ is the constant braking bias. At this point, the longitudinal force S (mainly) control the longitudinal dynamics, while the steering angle δ (mainly)control the lateral dynamics. We also consider that human drivers have limited rate of change of control variables and experimental results show that humans optimise their driving actions minimising the longitudinal and lateral jerks Viviani and Flash (1995),Bosetti et al. (2013),Biral et al. (2005). For this reason, it is assumed that longitudinal force and steering angle are not controlled directly, but via their time derivative, as follows:

$$\dot{S}=Mj_u\ , \quad \dot{\delta}=\omega_\delta \quad (15)$$

where j_u is the longitudinal jerk and ω_δ is the steering speed, which is approximately related to the lateral jerk. Summarizing, the vehicle vehicle dynamics is described by means of a set of 13 state variables:

$$\boldsymbol{x}=\{s,n,\alpha,u,v,w,\omega_x,\omega_y,\omega_z,N_r,N_f,S,\delta\}^T \quad (16)$$

and as many implicit first order differential equations, respectively (8), (9), (10), (12) and (15), which may be abbreviated to:

$$\hat{\boldsymbol{A}}\dot{\boldsymbol{x}}=\hat{\boldsymbol{B}}(\boldsymbol{x},\boldsymbol{u}) \quad (17)$$

where $\boldsymbol{u}$ are the inputs of the system:

$$\boldsymbol{u}=\{\omega_\delta,j_u\}^T \quad (18)$$

Equations (17) cannot be converted into the explicit form $\dot{\boldsymbol{x}}=\hat{\boldsymbol{A}}^{-1}\hat{\boldsymbol{B}}(\boldsymbol{x},\boldsymbol{u},t)$ because the matrix $\hat{\boldsymbol{A}}$ is singular, in other words equations (17) constitute a set of differential-algebraic equations (DAE) with *index* 1. Indeed, tire loads N_r, N_f are present into equations only as algebraic variables and they could be made explicit and eliminated from equations. However, this is not convenient because the remaining equations of motion would become much more complicated and computationally inefficient too. An alternative solution to the problem is to *relax* tire loads, i.e. to replace the algebraic variable with a differential form missing reference $N\rightarrow\tau_n\dot{N}+N$ and rewrite (10c) and (12a) as follows:

$$M(\dot{w}-\omega_y u+\omega_x v)=Mg+F_L(u) \\ -(\tau_n\dot{N}_r+N_r)-(\tau_n\dot{N}_f+N_f) \quad (19a)$$

$$I_{yy}\dot{\omega}_y+(I_{xx}-I_{zz})\omega_x\omega_z-I_{xz}\omega_z^2=h(S-F_f\delta) \\ +a(\tau_n\dot{N}_f+N_f)-b(\tau_n\dot{N}_r+N_r) \quad (19b)$$

According to these new equations, the load transfer between rear and front axle is not more instantaneous with the variation of the longitudinal force S, but has some lag which is proportional to the time constant τ_n. The relaxation of tire loads in not just an expedient used to reduce the equations DAE order, but it is also an approximation of the transfer load lag sue to the suspensions properties and the pitch inertia of the vehicle.

There are still other algebraic equations in the model, indeed (8) and (9) may be rewritten as follows:

$$\dot{s} = \frac{u\cos\alpha - v\sin\alpha}{1 - n\kappa(s)} \tag{20a}$$

$$\dot{n} = u\sin\alpha + v\cos\alpha \tag{20b}$$

$$\dot{\alpha} = \omega_z - \kappa(s)\frac{u\cos\alpha - v\sin\alpha}{1 - n\kappa(s)} \tag{20c}$$

$$w = n\tau(s)\frac{u\cos\alpha - v\sin\alpha}{1 - n\kappa(s)} \tag{21a}$$

$$\omega_x = [\tau(s)\cos\alpha + \upsilon(s)\sin\alpha]\frac{u\cos\alpha - v\sin\alpha}{1 - n\kappa(s)} \tag{21b}$$

$$\omega_y = [-\tau(s)\sin\alpha + \upsilon(s)\cos\alpha]\frac{u\cos\alpha - v\sin\alpha}{1 - n\kappa(s)} \tag{21c}$$

Equations (20) give the vehicle position and orientation s, n, α by integration of vehicle speeds u, v, ω_z, while (21) give algebraic explicit expressions of w, ω_x, ω_y that could be used to eliminate such variables from the other equations. Once again, variables elimination is not convenient from the computational point of view thus it is preferable to transform algebraic equations (21) into differential ones by relaxing speeds w, ω_x, ω_y with the substitution $w \to \tau_v\dot{w} + w, \omega_x \to \tau_v\dot{\omega}_x + \omega_x, \omega_y \to \tau_v\dot{\omega}_y + \omega_y$. In this case there is no physical justification for the velocity delay, therefore the relaxation time τ_v should be chosen as small as possible as trade off between numerical solution convergence robustness and solution accuracy. In conclusion, the system is described by means of equations (10), (12) and (20) which may be abbreviated to:

$$\tilde{\boldsymbol{A}}\dot{\boldsymbol{x}} = \tilde{\boldsymbol{B}}(\boldsymbol{x}, \boldsymbol{u}) \tag{22}$$

where $\tilde{\boldsymbol{A}}$ is now invertible. It is worth pointing out that only (10) and (12) are related to a specific vehicle model (the single track one), on the contrary (20) as well as their equivalent formulation (8), (9), (21), are only related to the road model and may be used in conjunction with any vehicle model.

4. OPTIMAL CONTROL PROBLEM

4.1 Vehicle dynamics in curvilinear abscissa domain

The minimum lap time problem consists in finding the vehicle control inputs that minimize the time T necessary to move the vehicle along the track from the starting line to the finish one, in other words the curvilinear abscissa s varies between fixed initial point $s = 0$ and end point $s = L$, while the final value T of the time variable t is unknown. For this reason, it is convenient to change the the independent variable from t to s in the equations of motion (22). Such variable change is based on the following derivation rule:

$$\dot{\boldsymbol{x}} = \frac{d\boldsymbol{x}}{dt} = \frac{d\boldsymbol{x}}{ds}\frac{ds}{dt}\boldsymbol{x'}\dot{s} = \boldsymbol{x'}\nu \tag{23}$$

Time domain equations (22) are then transformed in the space domain as follows:

$$\nu\tilde{\boldsymbol{A}}\boldsymbol{x'} = \tilde{\boldsymbol{B}}(\boldsymbol{x}, \boldsymbol{u}) \tag{24}$$

The first equation of (24) is algebraic and explicit the condition $\nu = \dot{s}$ given by (20a), therefore such equation must be eliminated, at the same time the variable s must be eliminated from the state vector $\boldsymbol{x}$. At this point the variable t is not more present in the mathematical model, however it can be obtained integrating the following equation:

$$\frac{\mathrm{d}t}{\mathrm{d}s} = t' = \frac{1}{\nu} = \frac{1 - n\,\kappa(s)}{u\cos\alpha - v\sin\alpha} \tag{25}$$

Summarizing, the s-domain state space model has 13 state variables:

$$\boldsymbol{y} = \{n, \alpha, u, v, w, \omega_x, \omega_y, \omega_z, N_r, N_f, S, \delta\}^T \tag{26}$$

and 2 inputs:

$$\boldsymbol{u} = \{j_u, \omega_\delta\}^T \tag{27}$$

while model equations may be summarized as a set of implicit differential equations:

$$\nu\boldsymbol{A}\boldsymbol{y'} = \boldsymbol{B}(\boldsymbol{y}, \boldsymbol{u}, s) \tag{28}$$

Equations (28) are not singular only and if only $\nu > 0$, i.e. the s-domain formulation cannot be used if the vehicle has to stop or revert the direction of travel on the track.

4.2 The Minimum Lap Time problem

The minimum lap time problem consists in finding the vehicle control inputs that move the vehicle from the starting line $s = 0$ to the finish one $s = L$ in the minimum time $T = t(L)$, while satisfying the mechanical equations of motion as well as other inequality constraints (tires adherence, max power, track width, etc.) Such optimal control problem (OCP) may be formulated as follows:

$$\text{find:} \quad \min_{\boldsymbol{u}\in\boldsymbol{U}} t(L) \tag{29a}$$

$$\text{subject to:} \quad \nu\boldsymbol{A}\boldsymbol{y'} = \boldsymbol{f}(\boldsymbol{y}, \boldsymbol{u}, s) \tag{29b}$$

$$\boldsymbol{\psi}(\boldsymbol{y}, \boldsymbol{u}, s) \le \boldsymbol{0} \tag{29c}$$

$$\boldsymbol{b}(\boldsymbol{y}(0), \boldsymbol{y}(L)) = \boldsymbol{0} \tag{29d}$$

where $\boldsymbol{y}$ and $\boldsymbol{u}$ are respectively the state variables and inputs vector, (29b) is the state space model in the s domain, (29c) are algebraic inequalities that may bound both the state variables and control inputs and (29d) is the set of boundary conditions used to (partially) specify the vehicle state at the beginning and at the end of the maneuver.

4.3 Inequality constraints and boundary conditions

Inequalities (29c) are used to keep the vehicle inside the admissible range of operating conditions. First of all, the vehicle must remain inside the track, i.e.:

$$-W_L(s) + c \le n \le W_R(s) - c \tag{30}$$

where $2c$ is the vehicle width, W_L, W_R are the distance of the left and right border from the track reference line, that possibly vary along the track. Additionally, tire forces must remain inside their ellipses of adherence:

$$F_r^2 + S_r^2 \le (\mu N_r)^2 \tag{31a}$$

$$F_f^2 + S_f^2 \le (\mu N_f)^2 \tag{31b}$$

where μ is the tires adherence coefficient and the vertical loads cannot become negative (i.e. no wheel lift from ground).

$$N_r \ge 0, \qquad N_f \ge 0 \tag{32}$$

The traction is limited by the maximum power P_{max} as follows:

$$Su \le P_{max} \tag{33}$$

The engine map can be introduced in the model but it is out of the scope of this work. Finally, the control inputs are bounded as follows:

$$-j_{u,max} \leq j_u \leq j_{u,max} \tag{34a}$$

$$-\omega_{\delta,max} \leq \omega_\delta \leq \omega_{\delta,max} \tag{34b}$$

Equations (30), (31), (33), (34) form a set of $m = 9$ unilateral constraints of type (29c). To complete the problem definition it is necessary to specify boundary conditions (29d). As the optimization is made on a closed loop track, it is natural to impose cyclic boundary conditions for all state variables $\boldsymbol{y}(s)$, except for the time t - where t(0)=0 while t(L) is free and under optimization.

4.4 Solution of the OCP problem

The OCP formulation(29) is general and the problem may be solved by using different approaches Bryson (1999) such as non-linear programming, dynamic programming, and Pontryagin's indirect method, which is the one that has been used in the present research. The OCP problem is particularly complicated due to the presence of inequality constraints (29c). However, it is possible to convert the constrained OCP problem into an unconstrained one by converting inequality constraints into penalty terms Bertolazzi et al. (2007), Bertolazzi et al. (2005) to be included in the optimality criterion (29a). Each penalty term should be very small (ideally null) when a constraint is satisfied and suddenly should become large as the constraint limit is approached and possibly reached. Therefore, the functional under minimization (29a) is replaced by the following one:

$$J = t(L) + \sum_{j=1}^{m} \int_0^L w_j \left(\psi_j \left(\boldsymbol{y}, \boldsymbol{u}, s\right)\right) ds \tag{35}$$

where penalties have been expressed in term of *wall* functions w_j. Equalities constraints (29b) are still present in the minimization problem, they may be eliminated by using the Lagrange's multipliers technique. More in detail, by defining the Hamiltonian function as follows:

$$H = \sum_{i=1}^{n} \lambda_i B_i \left(\boldsymbol{x}, \boldsymbol{u}, s\right) + \sum_{j=1}^{m} w_j \left(\psi_j \left(\boldsymbol{y}, \boldsymbol{u}, s\right)\right) = \boldsymbol{\lambda}^T \boldsymbol{B} + w(\boldsymbol{\psi}) \tag{36}$$

the constrained OCP problem (29) is converted into the *unconstrained* minimization of the functional:

$$J'\left(\boldsymbol{x}, \boldsymbol{u}, \boldsymbol{\lambda}, s\right) = t(L) + \int_0^L w(\boldsymbol{\psi}) + \boldsymbol{\lambda}^T \left(\boldsymbol{B} - \nu \boldsymbol{A} \boldsymbol{y}'\right) \, ds \tag{37}$$

According to variational first-principle, a necessary condition to minimize the functional $J'(\cdot)$ is the stationarity of the Hamiltonian (36), condition that leads to the following Two Point Boundary Value Problem (BVP):

$$\nu \boldsymbol{A} \boldsymbol{y}' = \boldsymbol{B}\left(\boldsymbol{y}, \boldsymbol{u}, s\right) \tag{38a}$$

$$\boldsymbol{N} \boldsymbol{y}' - \boldsymbol{A}^T \lambda' = -\partial_{\boldsymbol{x}}^T H \left(\boldsymbol{y}, \boldsymbol{u}, \boldsymbol{\lambda}, s\right) \tag{38b}$$

$$0 = \boldsymbol{b}\left(\boldsymbol{y}(0), \boldsymbol{y}(L)\right) \tag{38c}$$

$$0 = \partial_{\boldsymbol{y}_0}^T \boldsymbol{b} + \boldsymbol{A}\left(\boldsymbol{y}(0), s\right)^T \boldsymbol{\lambda}(0) \tag{38d}$$

$$0 = 1 + \partial_{\boldsymbol{y}_L}^T \boldsymbol{b} - \boldsymbol{A}\left(\boldsymbol{y}(L), s\right)^T \boldsymbol{\lambda}(L) \tag{38e}$$

$$0 = \partial_{\boldsymbol{u}}^T H \left(\boldsymbol{y}, \boldsymbol{u}, \boldsymbol{\lambda}, s\right) \tag{38f}$$

where $\boldsymbol{N} = \left(\partial_{\boldsymbol{y}}(\boldsymbol{A}^T \boldsymbol{\lambda}) - \partial_{\boldsymbol{\lambda}}(\boldsymbol{A}^T \boldsymbol{\lambda})\right)^T$. Equations (38c), (38d), (38e) are the set of boundary conditions on state variables and Lagrange multipliers. The equations change depending on the condition set for the state variables (i.e. on $\boldsymbol{b}\left[\boldsymbol{y}(0), \boldsymbol{y}(L)\right]$). Equations (38b) are the co-state equations and (38f) the equations for the optimal controls. Within Maple ©, the OCP problem is formulated according to equations (29) and then the BVP equations (38) are symbolically derived and discretized with a finite difference scheme. Finally the corresponding `C++` code is automatically generated ready to be compiled and numerically solved using `XOPtima` a specialised solver for the highly non linear system of equations deriving from the dicretized BVP problem Bertolazzi et al. (2007).

5. SIMULATION EXAMPLES

To prove the effectiveness of the proposed formulation, the minimum time manoeuvres of a sport vehicle running on 2D and 3D road models are here compared on three different type of road sections. The geometrical and inertial parameters of a Ferrari F430 has been used for simulations and reported in Table 1 (parameters which are not of public domain have been assumed consistently with the typical values of such car category). In the simulations to maximise the effect of the 3D road characteristics on the tyre vertical forces.

In the first example a straight road with a change in elevation of $5m$ down and then up is considered (see bottom plot of Figure 4) and to better analyse the influence of road slope on the axles' vertical loads the aerodynamic lift force is neglected $C_L = 0$. The vehicle is asked to accelerate from an initial velocity of $10m/s$ and run along the $600m$ straight in the minimum time ending with the same initial velocity. If the elevation is neglected the vertical loads show the usual load transfer to the rear, in the acceleration phase, and to the from in the braking phase. The slope change significantly affects the vertical loads as clearly expressed by relation (19a): the large load transfer due to the negative slope (see second plot from bottom of Figure 4) forces the optimal manoeuvre to slow down before entering in the down-hill and when "jumping" back on the flat straight in order to avoid to 'take off' (ie. reach zero vertical loads). Consequently the

Table 1. Vehicle characteristics

parameter	symbol	value
mass	M	1440 kg
CoG horizontal position	a	1.482 m
wheelbase	$a+b$	2.600 m
CoG height	h	0.42 m
roll inertia	I_{xx}	590 $\mathrm{kgm^2}$
pitch inertia	I_{yy}	50 $\mathrm{kgm^2}$
yaw inertia	I_{zz}	1730 $\mathrm{kgm^2}$
cross inertia	I_{xz}	1950 $\mathrm{kgm^2}$
width	c	1.760 m
power	P_{max}	440 kW
adherence coefficient	μ	1.2
rear cornering slip	K_r	29 $\mathrm{rad^{-1}}$
front cornering slip	K_r	29 $\mathrm{rad^{-1}}$
tire load relaxation time	τ_n	0.12 s
speed relaxation time	τ_n	0.01 s
aerodynamic drag	$1/2 \rho A C_D$	0.39 $\mathrm{Nm^{-2}s^2}$
aerodynamic lift	$1/2 \rho A C_L$	0.432 $\mathrm{Nm^{-2}s^2}$

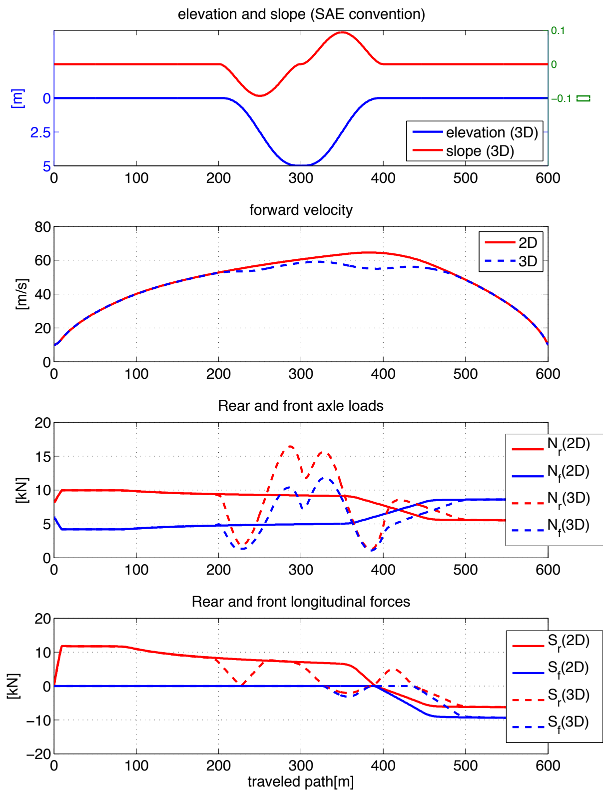

Fig. 4. Comparison between manoeuvres on flat straight and 3D straight (a down and up hill of $5m$ of elevation). Minimum time manoeuvre is $15.225s$ and $14.884s$ respectively for 3D and 2D road model (SAE convention, i.e z points downwards)

overall forward velocity is lower for the 3D case compared to the 2D as shown by second chart from top of Figure 4) and the manoeuvre time difference is $0.341s$.

The second example considers a U curve of $50m$ curvature radius, with positive banking of maximum $10°$ in the middle of the corner (see top plot of Figure 5) to analyse the effect of banking on maximum lateral acceleration ($C_L = 0$ also in this case). Similarly to the first example, the vehicle is asked to accelerate from an initial velocity of $10m/s$ and run along the $350m$ straight in the minimum time ending with the same initial velocity. As expected the positive banking allows to achieve higher lateral accelerations and velocities in the middle part of the curve (see middle and bottom plots of Figure 5). The manoeuvre time difference is $0.748s$. Additionally, the first and second charts of the Figure 5 shows that the use of road width is quite different between 2D and 3D.

The final example simulates a minimum lap time time with cyclic conditions on velocity, lateral position and forces (final conditions are equal to initial). The circuit geometry and elevation where derived from the information available at the circuit official website (http://www.mugellocircuit.it). Figure 6 top plot shows the trajectory for the 3D Mugello circuit with the color bar for the forward velocity in km/h. The bottom plot displays the circuit elevation and the middle plot compares the lateral accelerations The minimum time obtained with the flat mugello circuit is $1m\,1s\,160ms$ and for the 3D circuit is $1m\,2s\,160ms$. The lap time problem consists of about 100000 nonlinear equations (solved

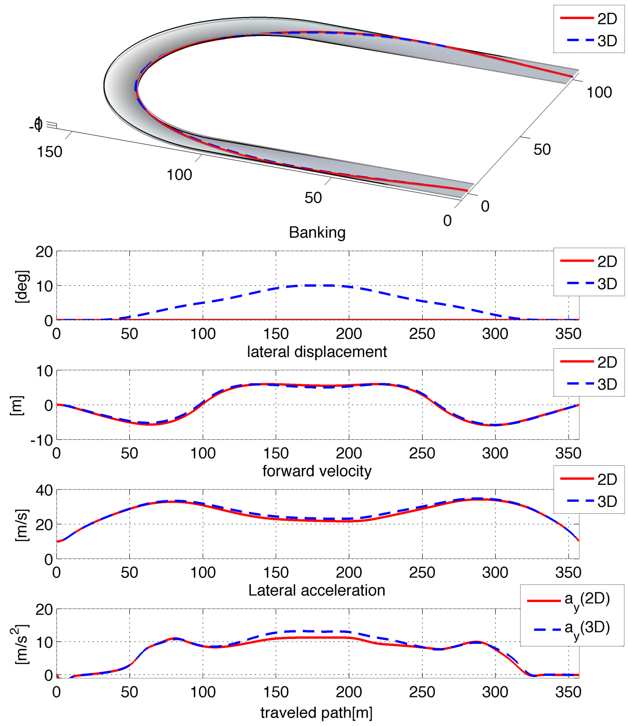

Fig. 5. Comparison between manoeuvres on flat and 3D U curve with internal banking. Minimum time manoeuvre is $13.660s$ and $14.039s$ respectively for 3D and 2D road model. Top chart compares trajectories (2D trajectory was projected on 3D road surface).

with a tolerance of $1e-09$) and the calculation time is of about $15s$ on a computer with a Intel Core i7 2.66GHz processor.

6. CONCLUSIONS

The optimal control and lap time optimization of vehicles such as racing cars and motorcycle is a challenging problem, the contribution of this paper is to provide a methodology which originally combines some modelling techniques for a numerically efficient problem formulation. First, the 3D road geometry is defined by using a minimum set of independent curvilinear coordinates which have the advantage that the vehicle position and orientation on the road is described in terms of state variables, without the need of additional tracking algorithm. Second, the equations of motion of the vehicle are derived with respect to a moving frame, yielding to equations which are simpler than the one derived in a fixed frame approach. Third, the time independent variable has been replaced by the road curvilinear abscissa, i.e. the equations of motion have been translated into the s position domain. This choice makes much more easier to numerically find the solution of the problem: working with a fixed mesh of time implies that a variation of the solution at the begin of the track must be propagated along the whole track, this problem is totally avoided by using a mesh fixed in space. Additionally, since time becomes a state variable and it turns out easier to formulate the minimum time problem. Fourth, an indirect method combined with a penalty formulation has been

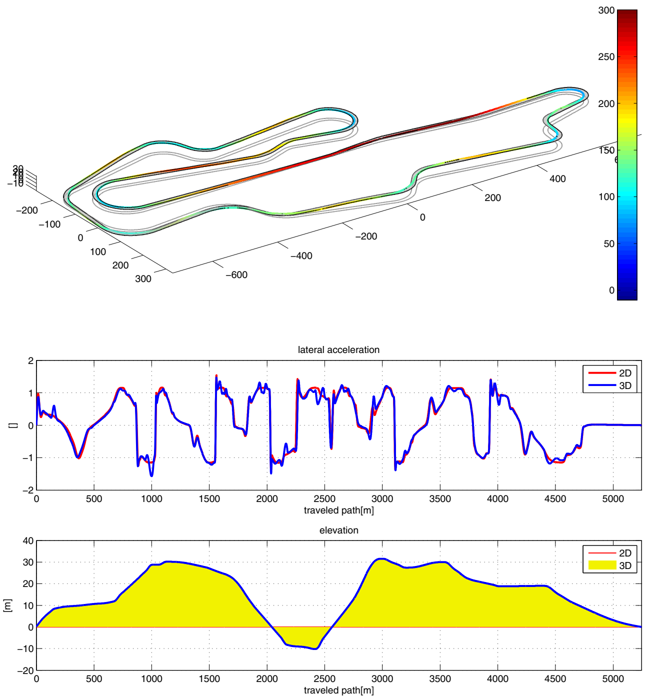

Fig. 6. Comparison between manoeuvres on flat and 3D Mugello circuit. Top plot shows trajectory and local velocity. Middle plot shows lateral acceleration normalized and bottom plot the circuit elevation.

used to convert the constrained minimization problem into un unconstrained one. Fifth, the Two Point Boundary Value problem generated by the indirect method, is first discretized with a finite different scheme and the large non-linear system of equations is solved with a custom developed library. The methods allows to solve a full circuit minimum lap time problem in less than one minute of cpu-computational time for complex vehicle models. The main drawback of the proposed method is probably due to the necessity of formulating equations of motion (38a) at symbolic level and to manipulate them to derive model co-equations (38b). However, the utilization of computer algebra tools, like *MBSymba* Lot and Lio (2004), makes this task affordable also for more realistic, complex vehicle models such as motorycles Cossalter et al. (1999) and Cossalter et al. (2013), rally cars Tavernini et al. (2013) 1999-Brysonand hybrid electric vehicles Lot and Evangelou (2013).

REFERENCES

Abe, M. (2009). *Vehicle Handling Dynamics*. Butterworth-Heinemann, Oxford.

Bertolazzi, E., Biral, F., and Da Lio, M. (2005). Symbolic-numeric indirect method for solving optimal control problems for large multibody systems: The time-optimal racing vehicle example. *Multibody System Dynamics*, 13(2), 233–252.

Bertolazzi, E., Biral, F., and Da Lio, M. (2007). Real-time motion planning for multibody systems: Real life application examples. *Multibody System Dynamics*, 17(2-3), 119–139.

Biral, F., Da Lio, M., and Bertolazzi, E. (2005). Combining safety margins and user preferences into a driving criterion for optimal control-based computation of reference maneuvers for an adas of the next generation. In *IEEE Intelligent Vehicles Symposium, Proceedings*, volume 2005, 36–41.

Blundell, M. and Harty, D. (2004). *The Multibody Systems Approach to Vehicle Dynamics*. Elsevier Butterworth-Heinemann, Burlington, MA, USA.

Bosetti, P., Lio, M., and Saroldi, A. (2013). On the human control of vehicles: an experimental study of acceleration. *European Transport Research Review*, 1–14.

Braghin, F., Cheli, F., Melzi, S., and Sabbioni, E. (2008). Race driver model. *Computers & Structures*, 86(13–14), 1503 – 1516.

Bryson, A.E. (1999). *Dynamic optimization*. Addison Wesley Longman.

Cossalter, V., Da Lio, M., Lot, R., and Fabbri, L. (1999). A general method for the evaluation of vehicle manoeuvrability with special emphasis on motorcycles. *Vehicle System Dynamics*, 31(2), 113–135.

Cossalter, V., Lot, R., and Tavernini, D. (2013). Optimization of the centre of mass position of a racing motorcycle in dry and wet track by means of the "optimal maneuver method". In *2013 IEEE International Conference on Mechatronics, ICM 2013*, 412–417.

Cui, L. and Dai, J. (2010). A darboux-frame-based formulation of spin-rolling motion of rigid objects with point contact. *Robotics, IEEE Transactions on*, 26(2), 383–388.

Gerdts, M. (2003). A moving horizon technique for the simulation of automobile test-drives. *ZAMM - Journal of Applied Mathematics and Mechanics / Zeitschrift für Angewandte Mathematik und Mechanik*, 83(3), 147–162.

Hans B., P. (2005). *Tire and Vehicle Dynamics, 2^{nd} edition*. SAE International.

Kehrle, F., Frasch, J., Kirches, C., and Sager, S. (2011). Optimal control of formula 1 race cars in a vdrift based virtual environment. In *Proceedings of the 18th IFAC World Congress, 2011*, volume 18, 11907–11912.

Kelly, D.P. and Sharp, R.S. (2010). Time-optimal control of the race car: a numerical method to emulate the ideal driver. *Vehicle System Dynamics*, 48(12), 1461–1474.

Kirches, C., Sager, S., Bock, H.G., and Schlöder, J.P. (2010). Time-optimal control of automobile test drives with gear shifts. *Optimal Control Applications and Methods*, 31(2), 137–153.

Lot, R. and Evangelou, S. (2013). Lap time optimization of a sports series hybrid electric vehicle. In *2013 World Congress on Engineering 2013, WCE 2013*.

Lot, R. and Lio, M. (2004). A symbolic approach for automatic generation of the equations of motion of multibody systems. *Multibody System Dynamics*, 12(2), 147–172.

Meirovitch, L. (2010). *Methods of Analytical Dynamics*. Dover Publications.

Tavernini, D., Massaro, M., Velenis, E., Katzourakis, D., and Lot, R. (2013). Minimum time cornering: the effect of road surface and car transmission layout. *Vehicle System Dynamics*. Article in Press.

Viviani, P. and Flash, T. (1995). Minimum-jerk, two-thirds power law, and isochrony: converging approaches to movement planning. *J. Exp. Psychol. Hum. Percept. Perform.*, 21(1), 32–53.